



# Supramolecular coordination complexes as diagnostic and therapeutic agents

Guocan Yu<sup>1,a</sup>, Meijuan Jiang<sup>1,a</sup>, Feihe Huang<sup>2,3</sup> and Xiaoyuan Chen<sup>4</sup>

## Abstract

The metal-based drugs represented by cisplatin, carboplatin, and oxaliplatin, prevail in cancer treatment, whereas new therapeutics are extremely slow to step into the clinic. Poor pharmacokinetics, multidrug resistance, and severe side effects greatly limit the development of metal-based anticancer drugs. The robustness and modular composition of supramolecular coordination complexes allow for the incorporation of novel diagnostic and therapeutic modalities, showing promising potentials for precise cancer theranostics. In this mini review, we highlight the recent advances in the development of supramolecular coordination complexes as diagnostic and therapeutic agents. The key focuses of these reports lie in searching sophisticated coordination ligands and nanoformulations that can potentially solve the issues faced by current metal-based drugs including imaging, resistance, toxicity, and pharmacological deficiencies.

## Addresses

<sup>1</sup> Laboratory of Molecular Imaging and Nanomedicine, National Institute of Biomedical Imaging and Bioengineering, National Institutes of Health, Bethesda, MD, 20892, United States

<sup>2</sup> State Key Laboratory of Chemical Engineering, Center for Chemistry of High-Performance & Novel Materials, Department of Chemistry, Zhejiang University, Hangzhou, 310027, PR China

<sup>3</sup> Green Catalysis Center and College of Chemistry, Zhengzhou University, Zhengzhou, 450001, PR China

<sup>4</sup> Yong Loo Lin School of Medicine and Faculty of Engineering, National University of Singapore, Singapore, 117597, Singapore

Corresponding authors: Chen, X ([chen9647@gmail.com](mailto:chen9647@gmail.com)); Huang, F ([fhuang@zju.edu.cn](mailto:fhuang@zju.edu.cn))

<sup>a</sup> These authors contributed equally.

Current Opinion in Chemical Biology 2021, 61:19–31

This review comes from a themed issue on **Bioinorganic Chemistry**

Edited by **Angela Casini** and **Ramon Vilar**

For a complete overview see the [Issue](#) and the [Editorial](#)

Available online 23 October 2020

<https://doi.org/10.1016/j.cbpa.2020.08.007>

1367-5931/Published by Elsevier Ltd.

## Keywords

Supramolecular coordination complex, Theranostics, Cancer, Metals in medicine.

## Introduction

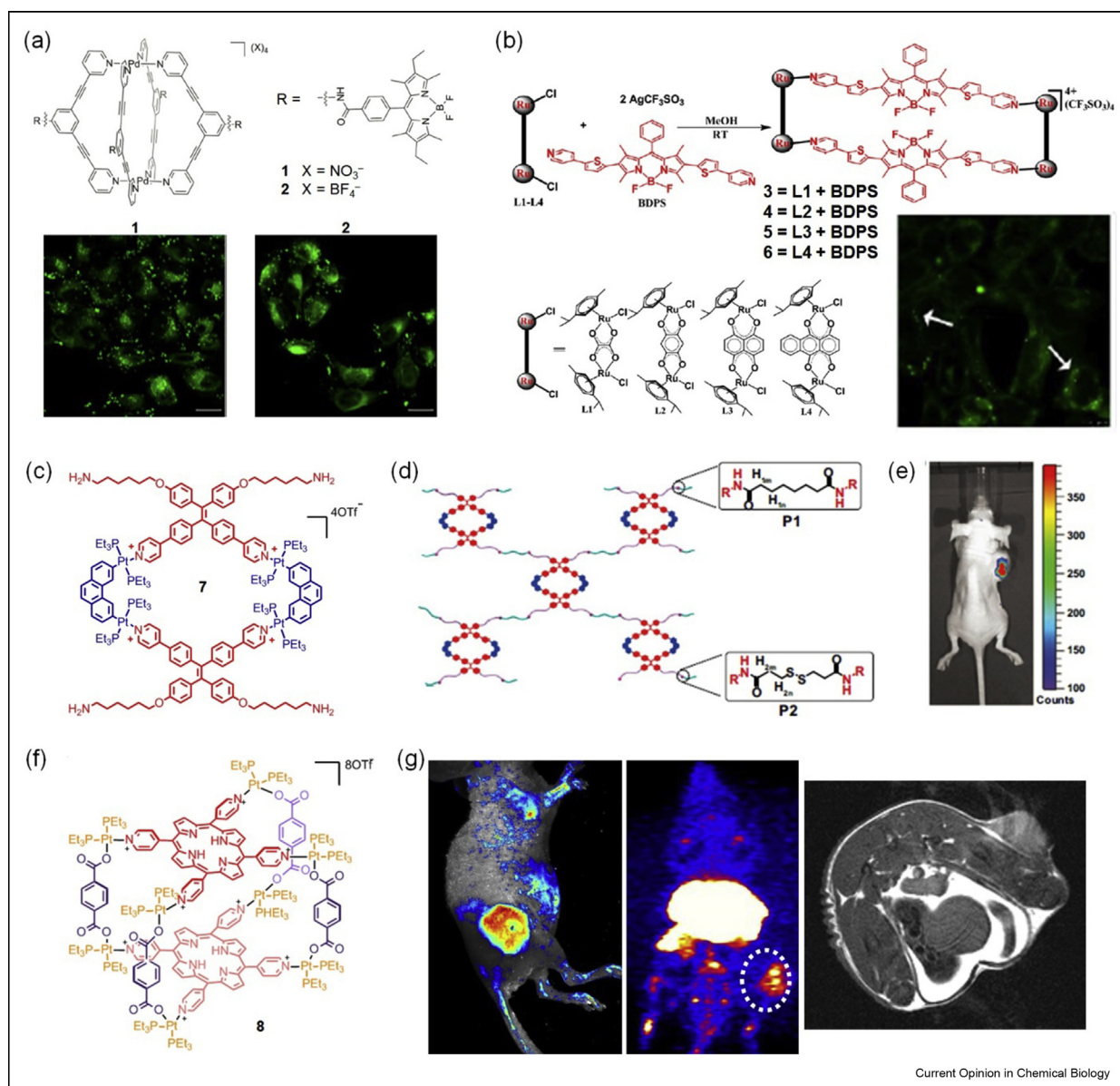
Cancer is fast becoming the leading cause of death worldwide, placing a heavy burden on patients, their families, and society [1–4]. Sophisticated drugs or nanoformulations that can specifically kill cancer cells, yet biocompatible to the normal tissues, are urgently needed for cancer patients. However, this goal is currently out of reach because of the considerable variations among tumor subpopulations and individuals [5,6]. Theranostics that integrates therapeutic and diagnostic capabilities into a single platform potentially meets the challenges for the next generation of personalized medicine. In these platforms, the diagnostic component reports the presence of tumors, their status, and their response to therapy, providing important information for the subsequent precise treatments [7–12]. However, such advances so far are mostly confined to the academic settings, with the majority of the reported theranostics incorporating the imaging and therapy independently rather than in an integrated platform, mismatching the diagnostic and therapeutic outputs. In addition, the therapeutic performances of the present drugs or nanomedicines are unsatisfactory in the clinic, prompting researchers to construct smart formulations synergistically combining multiple therapeutic modalities.

Since the serendipitous discovery of the antiproliferative capability of cisplatin by Barnett Rosenberg et al. in 1965, much effort has been devoted to exploring potent drugs on the basis of metal complexes for oncology therapy [13]. A large number of transition metal complexes including platinum (Pt<sup>II</sup> and Pt<sup>IV</sup>), gold (Au<sup>I</sup> and Au<sup>III</sup>), titanium (Ti<sup>IV</sup>), and ruthenium (Ru<sup>II</sup> and Ru<sup>III</sup>) have been extensively studied and evaluated, and some of them have entered clinical studies at different stages [13–16]. Still, most of these emerging therapeutic agents have encountered obstacles, such as low water solubility, poor pharmacological behaviors, unsatisfactory efficacy, severe side effects, and drug resistance. Fortunately, some of these drawbacks can be effectively solved by fully exploiting supramolecular coordination chemistry and nanotechnology using these therapeutic metal

complexes as building blocks [17–20]. Through the judicious choice of organic ligands and metal ions/clusters, discrete supramolecular coordination complexes (SCCs) with fascinating topologic structure have been fabricated *via* coordination-driven self-assembly [21,22]. More interestingly, diagnostic capability can be

introduced into these SCCs by using imaging probes as the coordination donors, facilitating noninvasive monitoring of the delivery, release, and excretion of the organometallic drugs with the assistance of fluorescence imaging, magnetic resonance imaging, positron emission tomography, or photoacoustic imaging [23,24]. By

Figure 1



(a) Chemical structures of the boron dipyrromethene (BODIPY)-modified Pd<sub>2</sub>L<sub>4</sub> metallacycles (1 and 2) and the confocal laser scanning microscope (CLSM) images of the cells culture with 1 and 2. Reproduced with permission from the study by Woods et al. [25], copyright 2019 Elsevier. (b) Chemical structures of the BODIPY-embedded metallacycles (3–6) and the CLSM images of the cells cultured with 5. Reproduced with permission from the study by Gupta et al. [26], copyright 2017 WILEY-VCH Verlag GmbH & Co. KGaA, Weinheim. (c) Chemical structure of the TPE-based metallacycle (7). (d) Illustration of crosslinked polymers constructed from the emissive TPE-based metallacycle. (e) The *in vivo* fluorescence image of the mouse injected with the nanomaterial prepared from the polymer (P2). Reproduced with permission from the study by Zhang et al. [35], copyright 2016 National Academy of Sciences. (f) Chemical structure of the porphyrin-based metallacycle (8). (g) NIR fluorescence, PET, and MRI images of the mice injected with the metallacycle-loaded nanoformulations. Reproduced with permission from the study by Yu et al. [37], copyright 2018 Nature Publishing Group. BODIPY, boron dipyrromethene; MRI, magnetic resonance imaging; NIR, near-infrared; PET, positron emission tomography; TPE, tetraphenylethane.

integrating other therapeutic agents into the SCCs, the anticancer properties of the resultant formulations are vastly improved by combining chemotherapy with photodynamic therapy (PDT) and photothermal therapy. Herein, we highlight the recent developments of SCCs in cancer theranostics aiming to point out some pivotal tendency in potential applications of the reported supramolecular structures.

### Incorporation of diagnostic functions into SCCs

The inspiration for the employment of SCCs in biomedical applications arises from their awesome merits of (i) the ease of fine-tuning the topological structures of the coordination complexes, (ii) the plentiful choices of metal ions or clusters with changeable sizes and angles, (iii) the feasible integration of specific agents with fascinating functions *via* pre-modifications or postmodifications. Imaging probes can be incorporated into SCCs for *in vitro* and *in vivo* imaging to trace their delivery and excretion. Various strategies have been exploited to achieve this goal, such as chemical modification, direct coordination self-assembly, physical encapsulation, and host–guest recognition.

Fluorophores with high quantum yield (QY) could be conjugated to the coordination building block, thus introducing imaging capability into SCCs. For example, Woods et al. [25] conjugated highly emissive boron dipyrromethene (BODIPY) moieties to the 3,5-bis(3-ethynylpyridine)phenyl scaffold and obtained luminescent Pd<sub>2</sub>L<sub>4</sub> metallacages (**1** and **2**). The bright fluorescence arising from BODIPY allowed for monitoring the cellular uptake and subcellular localization of the metallacages and found that the internalization was driven by active transportation and the metallacages accumulated in cytoplasmic vesicles (Figure 1a).

Fluorescent probes with rigid structures are inherent coordination donors when modified with carboxylate or pyridine groups, such as BODIPY, tetraphenylethane (TPE), and porphyrins. Gupta et al. [26] constructed thiophene-based BODIPY Ru(II) rectangles (**3–6**) using dinuclear arene-ruthenium precursors and a thiophene-functionalized dipyridine BODIPY ligand, and the intracellular distribution of this metallacycle was visualized by the net fluorescence of BODIPY (Figure 1b). Pd(II)- and Pt(II)-cornered square-planar complexes were also used by Gupta et al. [27] and Zhou et al. [28] to fabricate BODIPY-based fluorescent triangles and rectangles. The characteristic fluorescence of the BODIPY cores allowed intracellular visualization of these metallacycles by using a confocal microscope. Ma et al. [29] constructed three highly fluorescent metallacycles utilizing a near-infrared (NIR)–emissive dipyrindyl ligand and Pt(II) precursors with different

shapes. Interestingly, the formation of D- $\pi$ -A structures due to the introduction of two electron donors to the cyanostilbene-based backbone shifted the emission of the ligand to 735 nm. These metallacycles combining both imaging and therapeutic abilities offered a new type of theranostics toward cancer management. Notably, the anticancer ability of the metal-acceptors was greatly maintained by the formation of SCCs, the IC<sub>50</sub> values of these SCCs were comparable with or even lower than cisplatin.

Different from traditional fluorophores suffering from aggregation-caused quenching, TPE derivatives exhibit a unique aggregation-induced emission (AIE) phenomenon at concentrated states through the restriction of intramolecular rotation [30,31]. Interestingly, the intramolecular rotation could be hindered by the formation of SCCs through coordinations, making the metallacomplexes highly emissive even in diluted states [32–34]. Zhang et al. [35] prepared a rhomboidal TPE-based metallacycle (**7**) and further crosslinked the fluorescent metallacycle-cored polymers *via* bifunctional covalent linkages (Figure 1c and d). Benefiting from the AIE effect, nanoparticles prepared from these supramolecular polymers were used as contrast agents for cell imaging and *in vivo* fluorescence imaging (Figure 1e). Yu et al. [36] synthesized a TPE-based metallacage *via* multiple-component coordination, exhibiting bright emission as a result of AIE effect. The stability of this theranostic SCC was significantly improved by encapsulation into the nanoparticles formed from two lipid–polymer conjugates. The delivery process was detected in real-time by exploiting the AIE feature of this metallacage. Based on both enhanced penetration permeability and retention (EPR) effect and active targeting ability, this nanomedicine highly accumulated in tumor tissue, which enhanced antitumor efficacy and reduced systemic toxicity.

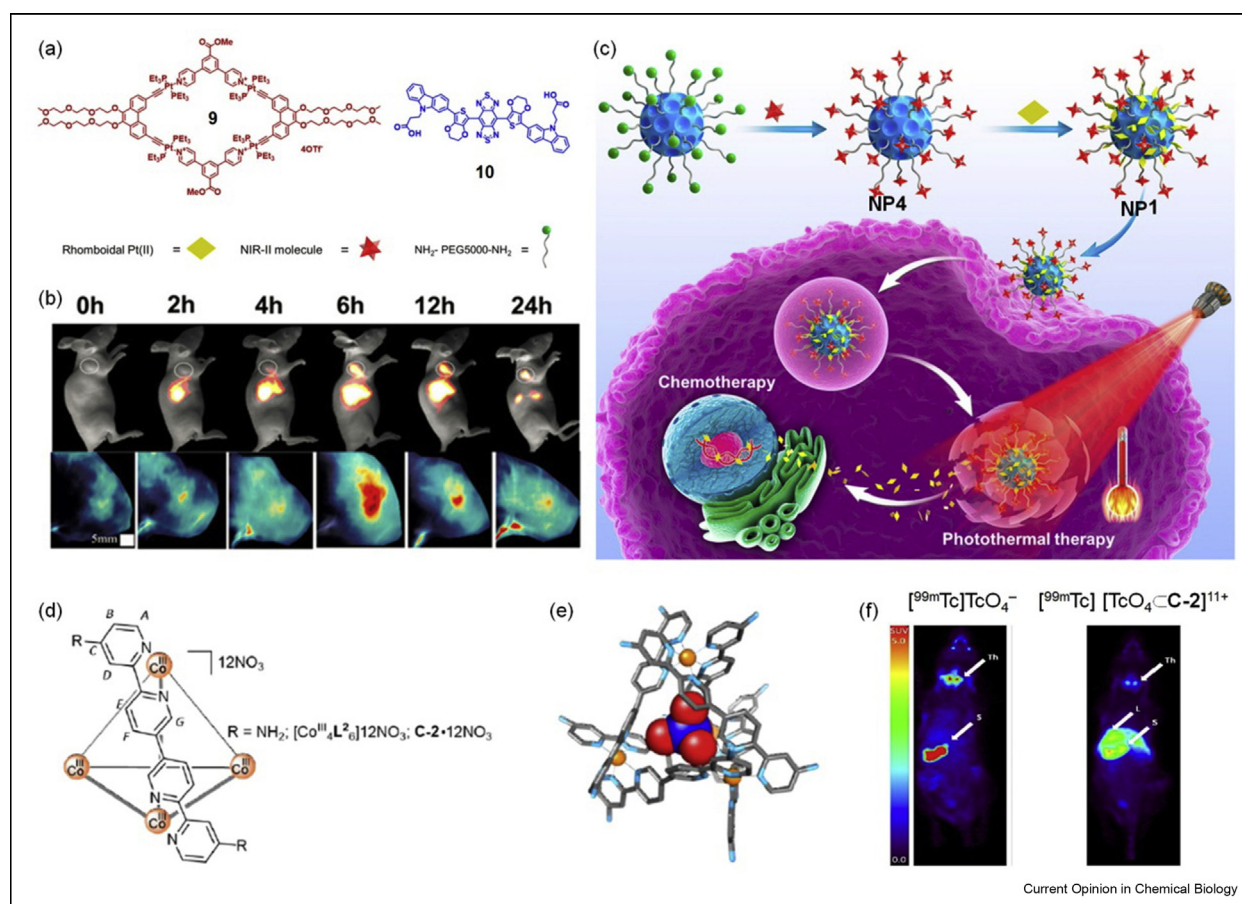
Porphyrin is a classic fluorophore, while the fluorescence is remarkably quenched by the  $\pi$ - $\pi$  stacking of the hydrophobic core. Although various modifications have been conducted by introducing water-soluble segments aiming to improve their solubility, it remains a challenge to realize single molecular dispersion. Yu et al. [37] inserted 5,10,15,20-tetra(4-pyridyl)porphyrin (TPP) into the metallacage (**8**) as top and bottom faces through a multicomponent coordination-driven self-assembly (Figure 1f). The distance between the fluorophores was mechanically elongated. In this way, the intermolecular  $\pi$ - $\pi$  stacking of TPP was remarkably suppressed, significantly enhancing the fluorescence. Metallacage-loaded nanoparticles were obtained, and their *in vivo* delivery was traced by NIR fluorescence imaging. More intriguingly, the porphyrin cores of the metallacage were suitable hosts for magnetic Mn<sup>2+</sup> and radioactive <sup>64</sup>Cu<sup>2+</sup> ions, which allowed the implementation of

magnetic resonance imaging and positron emission tomography imaging with high sensitivity and resolution (Figure 1g). The nanoparticles with trimodality imaging allowed precise diagnosis of tumors and tracing of the delivery, organ distributions, and excretion of the nanoparticles.

NIR-II imaging holds promise to provide information of tumor location and progression attributing to its low interfering signal, deep penetration, and the high signal-to-background ratio. Inspired by these superb merits from the NIR-II over the NIR-I window for *in vivo* imaging, Sun et al. [38] developed a series of theranostics through physical encapsulation. For example, ternary theranostic nanoparticles comprising of a rhomboidal metallacycle, a NIR-II probe and an amphiphilic copolymer were prepared [38]. This theranostic system possesses excellent photostability for accurate diagnosis

of cancer with high resolution and signal-to-noise ratios. Similarly, a nanococktail was prepared by loading an organic NIR-II dye and an organoplatinum(II) metallacycle into the polymeric nanoparticles self-assembled from Pluronic F127 [39]. This nanococktail exhibited high photostability and negligible background in the NIR-II region, showing unparalleled advantages for real-time monitoring the process of therapy. Moreover, the same group also engineered a dual-modal theranostic nano-agent by incorporating discrete Pt(II) metallacycle (9) and NIR-II dye (10) into multifunctional melanin dots (Figure 2a) [40]. Both NIR-II imaging and photoacoustic imaging confirmed accumulation of the nano-agent (NP1) in the tumor region (Figure 2b), which allowed for image-guided chemophotothermal therapy (Figure 2c). It should be emphasized that the coordination self-assembly and nanoformulations did not diminish the anticancer activity of the

Figure 2



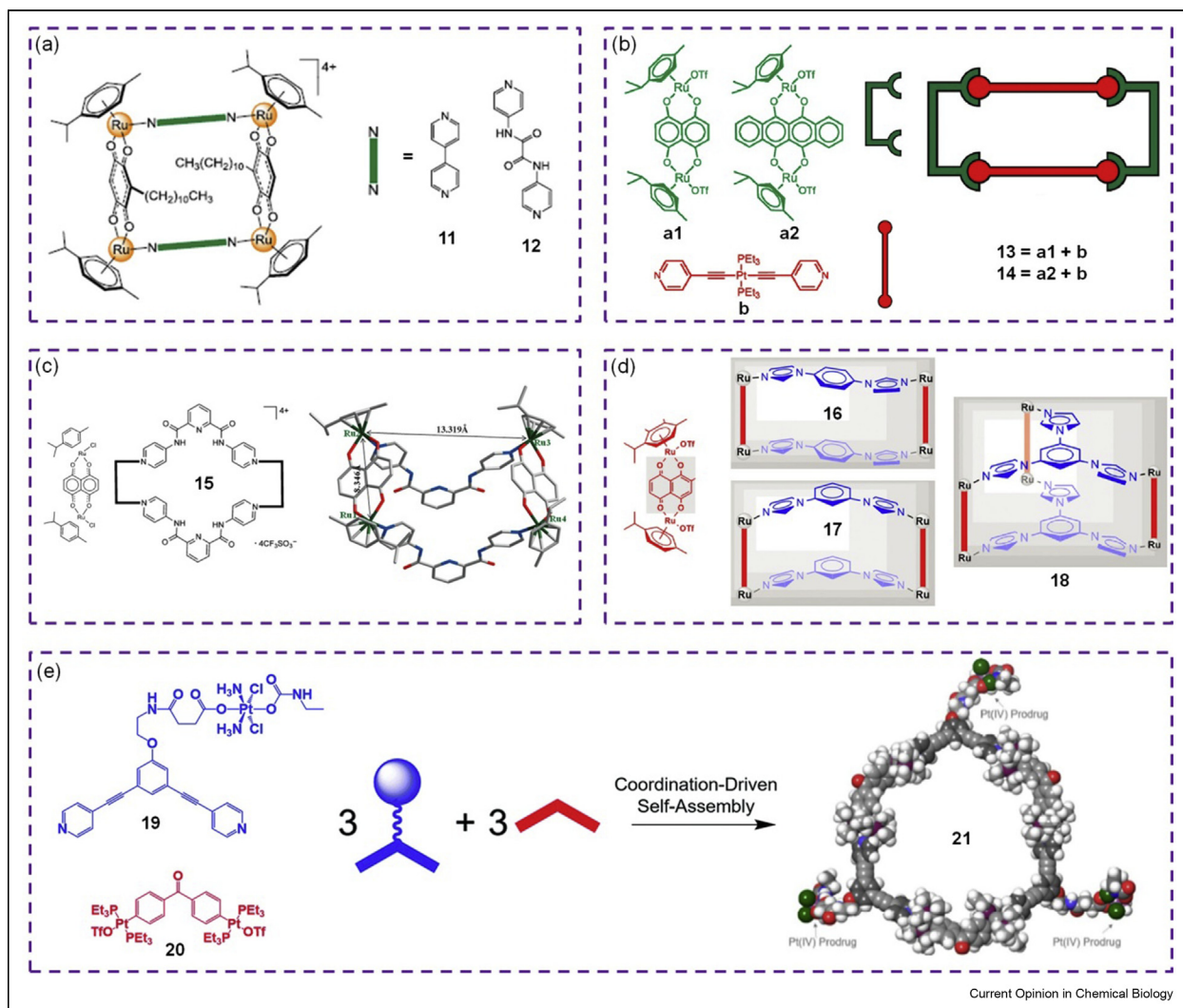
(a) Structures of discrete metallacycle **9** and NIR-II molecular dye **10**. (b) NIR-II fluorescence and photoacoustic images of the mice bearing U87MG tumors at different times post tail vein injection of NP1. (c) The schematic diagram of nanotheranostic NP1 for chemophotothermal synergistic therapy. Reproduced with permission from the study by Sun et al. [40], copyright 2019 National Academy of Sciences. (d) Chemical structure of C-2. (e) Single-crystal structure of [ReO<sub>4</sub>-C-2]<sup>11+</sup>. (f) SPECT images of the mice injected with free [<sup>99m</sup>Tc]TcO<sub>4</sub><sup>-</sup> and [<sup>99m</sup>Tc][TcO<sub>4</sub>-C-2]<sup>11+</sup>. Reproduced with permission from the study by Burke et al. [44], copyright 2018 American Chemical Society. NIR, near-infrared; SPECT, single-photon emission computed tomography.

organoplatinum(II) precursors in these cases, and additional photothermal therapy arising from the carriers even elevated the therapeutic efficacy.

Metallacages with hollow cavity are able to complex diagnostic guests, making the host–guest recognition an effective method to visualize the metallacages. Freudenreich et al. [41] and Garci [42] constructed water-soluble arene-ruthenium metallacages and used them as supramolecular hosts to encapsulate hydrophobic porphyrin. The cellular endocytosis of the supramolecular complexes and release of porphyrin after internalization

into the cells were fully investigated by fluorescence imaging. Yu et al. [43] also used a discrete organoplatinum(II) metallacage with a well-defined cavity as a supramolecular host to load octaethylporphine and further encapsulated the host–guest complex into polymeric nanoparticles for fluorescence image-guided chemophotodynamic therapy. Burke et al. [44] synthesized a tetrahedral  $\text{Co}^{\text{III}}_4\text{L}_6$  (**C-2**), which exhibited high binding affinity towards  $\gamma$ -emitting  $^{99\text{m}}\text{Tc}[\text{TcO}_4^-]$  anion (Figure 2d). The association constant was as high as  $61,000 \text{ M}^{-1}$  between this metallacage host and pertechnetate analog (perhenate,  $\text{ReO}_4^-$ ) (Figure 2e).

Figure 3



(a) Chemical structures of the Ru-based metallacycles (**11** and **12**). Reproduced with permission from the study by Gupta et al. [45], copyright 2015 Elsevier. (b) Chemical structures and cartoon illustration of the preparation of metallacycle (**13** and **14**). Reproduced with permission from the study by Vajpayee et al. [46], copyright 2011 American Chemical Society. (c) Chemical and single-crystal structure of the metallabowl (**15**). Reproduced with permission from the study by Mishra et al. [51], copyright 2014 Wiley-VCH Verlag GmbH & Co. KGaA, Weinheim. (d) Chemical structures of the metallacycles (**16** and **17**) and metallacage (**18**) self-assembled from the  $0^\circ$  Ru clip and ditopic/tritopic imidazole-based ligands. Reproduced with permission from the study by Zhao et al. [52], copyright 2019 National Academy of Sciences. (e) Illustration of the self-assembly of the hexagon (**21**) using **19** and **20** as building blocks. Reproduced with permission from the study by Yue et al. [56], copyright 2018 Royal Society of Chemistry.

Subsequent single-photon emission computed tomography imaging indicated that the capsule remained intact during imaging (Figure 2f). Compared with the thyroid accumulating free oxo-anion, *in vivo* imaging also indicated dramatic variations in the distributions of the complex.

### SCCs for cancer therapy

By using Pt, Pd, Rh, Ru, and Ir as the coordination acceptors, Therrien, Stang, Chi, Casini et al. developed a series of two dimensional metallacycles (*e.g.* triangles, rectangles, rhomboids, and hexagons) and 3D metallacages for cancer therapy [24]. These SCCs exhibited antiproliferative effects against various cancer cell lines. The potency of partial SCCs is similar to and, in some cases, even better than the commercially used cisplatin, carboplatin, and oxaliplatin. The anticancer mechanisms of these SCCs mainly include membrane damage, autophagy, DNA damage, cell apoptosis, and increased p53 expression.

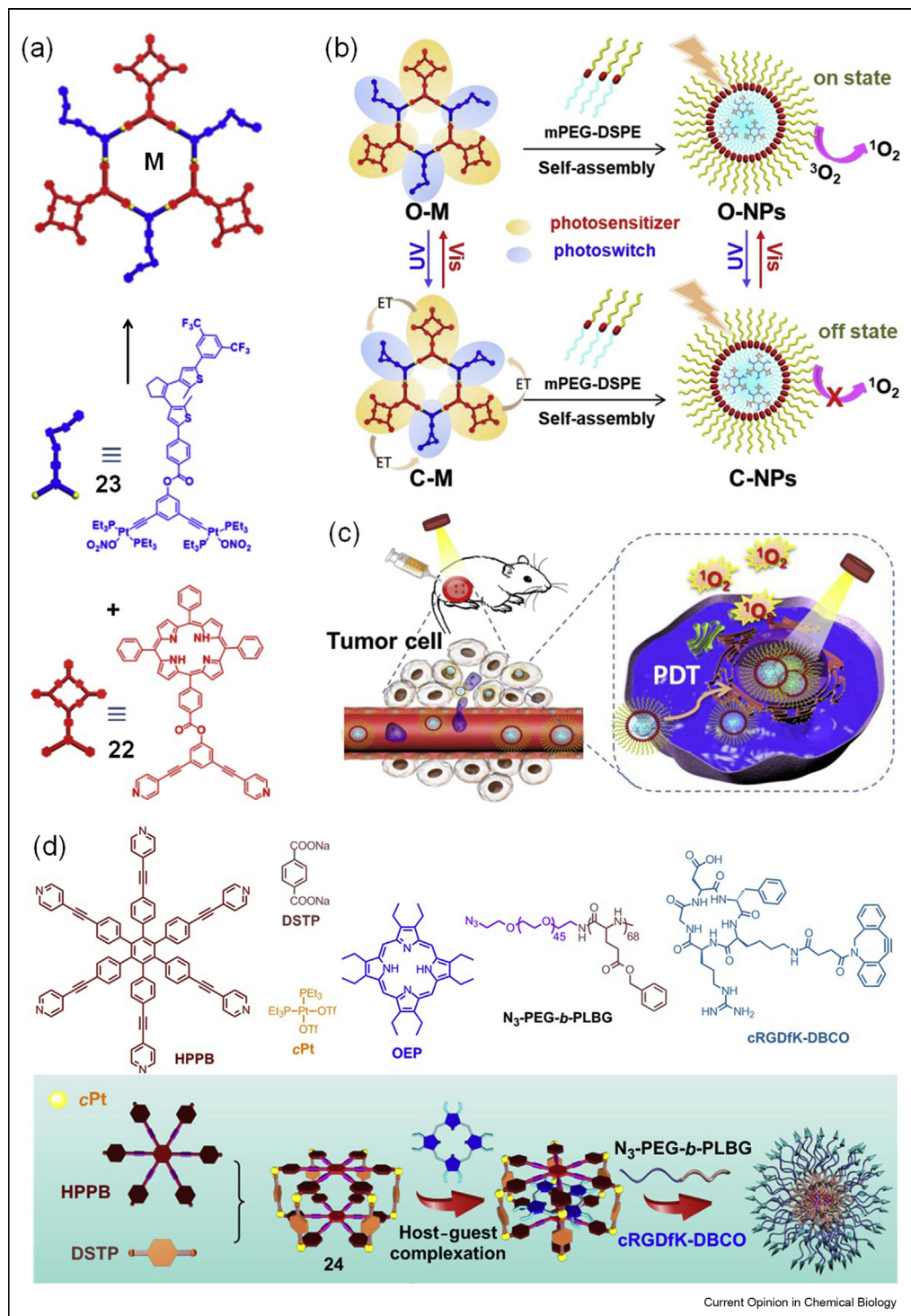
Biological activity of Ru-based complexes prompt analogous studies of Ru(II)-arene SCCs with particular interest in their anticancer performance. Supramolecular Ru(II) metallacycles displayed some exciting advantages, such as relatively high solubility and stability in aqueous solution. Gupta et al. [45] designed Ru(II)-arene metallarectangles (**11** and **12**) that showed exciting potency to cancer cells rather than normal cells. These metallacycles were highly toxic against human ovarian cancer cells (Figure 3a) [45]. Vajpayee et al. [46] (Figure 3b). Various Ru(II)-arene metallabowls, Ru(II)-arene [2] catenane, and 3D Ru(II) metallacages have been constructed, and their antiproliferative capabilities were evaluated against a panel of cancer cells [47–51]. The metallabowl (**15**) featuring 5,8-dihydroxy-1,4-naphthaquinonato ligands was twice as potent as doxorubicin (DOX) and cisplatin against HCT-15 cells (Figure 3c) [51]. Zhao et al. [52] synthesized a series of Ru(II)-arene rectangles (**16** and **17**) and trigonal prisms (**18**) self-assembled from bidentate or tridentate imidazole-based ligands with *p*-cymene ruthenium (II) acceptors (Figure 3d). *In vitro* anticancer studies demonstrated that only the SCCs containing 5,8-dihydroxy-1,4-naphthaquinonato-based scaffolds exhibited satisfactory effect. The screened SCCs displayed pronounced selectivity for HepG-2 cells over the healthy cells.

Mishra et al. [53] prepared two tetracationic Pt(II) and Pd(II) metallacycles from an *N,N'*-bis(4-[pyridin-4-ylethynyl]phenyl)pyridine-2,6-dicarboxamide and *cis*-blocked metal complexes. Both metallacycles exhibited antiproliferative effect, especially for the Pt(II) metallacycle, which was more potent than cisplatin against head and neck and thyroid cancer cells, while less toxic against normal cells. Gupta et al. [27] reported Pd(II)-

based supramolecule complexes with triangular/square architectures using BODIPY derivatives as ligands. Notably, these SCCs were more potent against glioblastoma cells than normal lung fibroblasts, and their anticancer efficacy was even higher than that of cisplatin against the glioblastoma cells. McNeill et al. [54] investigated the influence of different ligands on the biological activity of Pd<sub>2</sub>L<sub>4</sub> helicates. Their study showed that the antiproliferative results of the SCCs were correlated with the stability in biological media. Among them, Pd<sub>2</sub>L<sub>4</sub> (L = 1,3-bis-hexane triazole phenyl) helicates possessed the highest anticancer effect, *e.g.* it was seven-fold more potent than cisplatin against resistant MDA-MB-231 cells. The anticancer mechanism of this SCC is also different from that of cisplatin through DNA crosslinks; it triggers cell apoptosis by disrupting the cell membrane.

Attributing to their inherent anticancer capability, platinum-based complexes have attracted extensive attentions over the past decades. Stang et al. developed large libraries of mononuclear and multinuclear platinum acceptors with different angles and sizes and further constructed a large number of metallacycles and metallacages [24]. *In vitro* and *in vivo* evaluations confirmed excellent anticancer output of these SCCs against various cancer cell lines. For example, Grishagin et al. [55] designed an endohedral amine-functionalized rhomboid using 2,6-bis(pyrid-4-ylethynyl) aniline and 2,9-bis(*trans*-Pt[PEt<sub>3</sub>]<sub>2</sub>NO<sub>3</sub>) phenanthrene as building blocks. *In vivo* antitumor evaluations indicated that the mice treated with this metallarhomboid resulted in a substantial 64% reduction of the tumor burden. Recently, Yue et al. [56] reported a Pt<sub>3</sub>L<sub>3</sub> hexagon (**21**) through the coordination between a Pt(IV) prodrug-conjugated dipyrindyl ligand (**19**) and a bidentate ligand (**20**) (Figure 3e). Through this supramolecular method, three equivalents of cisplatin could be delivered into the cancer cells by the reduction of the Pt(IV) prodrug. Compared with free cisplatin, higher cellular uptake was realized for the metallacycle, effectively improving the anticancer efficacy against a range of cancer cells. To improve the anticancer results and overcome drug resistance, other therapeutic modalities were introduced into the SCCs through covalent and noncovalent ways. For example, Zhou et al. [28], Zhou et al. [57,59] and Yao et al. [58] reported the preparation of metallacycles containing porphyrin-based, Ru complex-based, or BODIPY-based photosensitizers. The combination of chemotherapy and PDT greatly enhanced the anticancer performance of these metallacycles. Apart from metallacycles and metallacages, metallohelices with different topological structures and mechanisms of action were developed and applied as anticancer agents. For example, Brabec et al. [60] used Fe as the coordination acceptor to prepare a series of M<sub>2</sub>L<sub>3</sub> helicates, which exhibited higher potency than cisplatin against HCT116 p53<sup>+/+</sup> cell line in nM range. They pointed out

Figure 4



(a) Self-assembly of the metallacycle (M). (b) Illustration of the controllable  $^1\text{O}_2$  generation M and nanoparticles. (c) Illustration of nanomedicine delivery followed by the EPR effect and PDT effect. Reproduced with permission from the study by Qin et al. [63], copyright 2019 American Chemical Society. (d) Chemical structures of the building blocks (HPPB, DSTP, cPt, OEP,  $\text{N}_3$ -PEG-*b*-PLBG, and cRGDFK-DBCO) and cartoon illustration of the nanomedicine preparation. Reproduced with permission from the study by Yu et al. [43], copyright 2019 National Academy of Sciences. EPR, enhanced penetration permeability and retention; PDT, photodynamic therapy.

the binding strength and number of binding sites of metallohelicenes played important roles in the interaction with oligonucleotide duplexes with bulges, and these interactions were dependent on the size of the bulge that finally determine their efficacy. Faulkner et al. [61] further reported the preparation of the stereoselective asymmetric metallohelicenes possessing antiparallel head-to-head-to-tail 'triplex' strand arrangement. Interestingly, these self-assemblies exhibited structure-dependent anticancer activity against the HCT116 p53<sup>++</sup> cell line, remarkably changing the cell cycle while merely damaging the DNA structures.

### Nanofabrications from SCCs

For *in vivo* antitumor applications, the stability in the physiological environment and pharmacokinetic behaviors of the SCCs should be optimized to improve efficacy while reducing side effects. Nanotechnology was used to overcome the barriers faced by SCCs during their delivery and action processes. Yu et al. [62] encapsulated an AIE metallacage into nanoparticles as cancer theranostics. Attributing to the EPR effect and targeting ability, the circulation time of the nanomedicine was greatly prolonged and its tumor accumulation was significantly increased. This nanomedicine exhibited better antitumor results than those of the commercial platinum-based drugs including oxaliplatin, carboplatin, and cisplatin. The administration of nanomedicine achieved more durable tumor suppression and apoptosis of tumor cells, while the side effects of the chemotherapeutic agents toward normal tissues were much reduced. Stang and coworkers conjugated glutathione-responsive copolymers to an AIE metallacage to afford an amphiphilic drug carrier [62]. Nanoparticles self-assembled from this material were able to load neutral DOX in the hydrophobic cores. A dual-responsive drug release was achieved because of the degradation of the carrier triggered by the high glutathione and the protonation of the DOX by the low pH inside cancer cells. *In vivo* studies confirmed that the NPs 50 nm in diameter were capable of codelivering platinum-based anticancer drugs and DOX in a synergistic pattern, which effectively suppressed tumor growth. Sun et al. [38,40] and Ding et al. [39] co-loaded metallacages and NIR probes into the polymeric nanoparticles and melanin dots for tumor diagnosis and NIR-II image-guided therapy. Attributing to the sophisticated design and advantages from nanotechnology, the therapeutic efficacy of these theranostic systems was greatly improved; the tumors were completely ablated by the chemophotothermal synergistic therapy.

Qin et al. [63] controlled the generation of singlet oxygen (<sup>1</sup>O<sub>2</sub>) by light through the conjugation of porphyrin (**22**) and diarylethene moieties (**23**) to a

metallacycle (**M**) (Figure 4a). In this light-responsive dual-stage metallacycle, the production of <sup>1</sup>O<sub>2</sub> was completely inhibited while the diarylethene groups were in the ring-closed form (**C-M**), while efficient generation of <sup>1</sup>O<sub>2</sub> was realized when these units were converted to the ring-open form (**O-M**) (Figure 4b). The metallacycle was further encapsulated by 1,2-distearoyl-*sn*-glycero-3-phosphoethanolamine-*N*-methoxy(polyethylene glycol) (mPEG-DSPE) to obtain a nanomedicine, which allowed for efficient delivery to cancer cells through EPR effect (Figure 4c). The switchable dual-stage nanomedicine was able to ablate the tumors through controllable light irradiation.

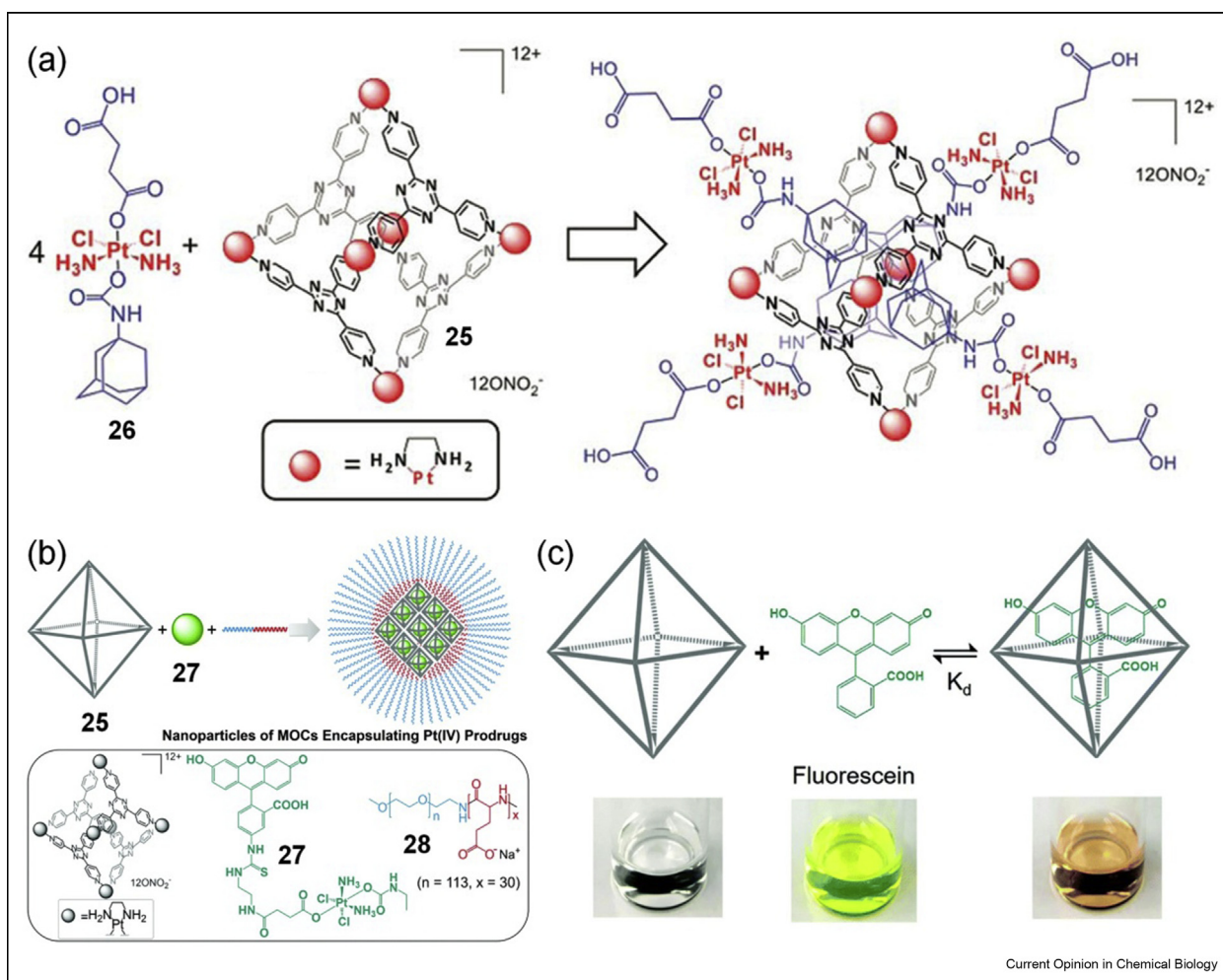
Biological activity of Ru-based complexes prompt analogous studies of Ru(II)-arene SCCs with particular interest in their anticancer performance. Supramolecular Ru(II) metallacycles displayed some exciting advantages, such as relatively high solubility and stability in aqueous solution. Therrien *et al.* designed Ru(II)-arene metallarectangles (**11** and **12**) that showed exciting potency to cancer cells rather than normal cells. These metallacycles were highly toxic against human ovarian cancer cells because of the severe  $\pi$ - $\pi$  stacking. As discussed above, the TPP-based metallacage developed by Yu et al. [37] overcame this obstacle, greatly improving the <sup>1</sup>O<sub>2</sub> generation QY by increasing the intersystem crossing efficiency of the photosensitizer. PEGylation of the metallacage by mPEG-*b*-PEBP and RGD-PEG-*b*-PEBP endowed the nanomedicine with prolonged blood circulation time and less nonspecific tissue uptake. This nanoformula had a phototoxicity index as high as 246, indicating that the phototherapy could be spatiotemporally controlled by the laser. *In vivo* studies demonstrated the combination of chemotherapy, and PDT possessed outstanding anticancer performances in fighting against U87MG, drug-resistant A2780CIS, and orthotopic tumors, effectively preventing tumor recurrence and metastasis after a single treatment. Yu et al. [43] used a discrete metallacage (**24**) as a supramolecular host to complex a photosensitizer (**OEP**) through host-guest chemistry to form a dual functionalized system, which was further encapsulated into the nanoparticles to afford a nanomedicine (Figure 4d). This nanoformulation specifically delivered the chemotherapeutic drug and photosensitizer to cancer cells, realizing synergistic effect against the drug-resistant cancer cells. *In vivo* antitumor studies confirmed that the combination of chemotherapy and PDT eradicated the drug-resistant tumors, confirming the superior antitumor ability of this nanomedicine. Compared with other delivery vehicles, the excellent compatibility and biodegradability of the polymeric carriers used in these supramolecular systems make these nanomedicines more likely to be clinically translatable.

### Host–guest chemistry using cucurbit

Chemotherapy often results in tumor relapse and drug resistance, which are the main obstacles to improving life quality and prolonging survival of the patients. The cocktail strategy combining different drugs with distinct anticancer mechanisms is an attractive choice to boost anticancer results. Three-dimensional SCCs with unique cavities are interesting supramolecular hosts, which are able to complex with diagnostic or therapeutic guests through host–guest recognitions, thus realizing synergistic therapeutic efficacy. Zheng et al. [64] developed a well-defined  $M_6L_4$  metallacage (**25**) and used it as a drug delivery system (Figure 5a). Host–guest complexation between the cage and adamantyl groups derived association of four Pt(IV) prodrugs (**26**) within each cage. The highly positive charge of the

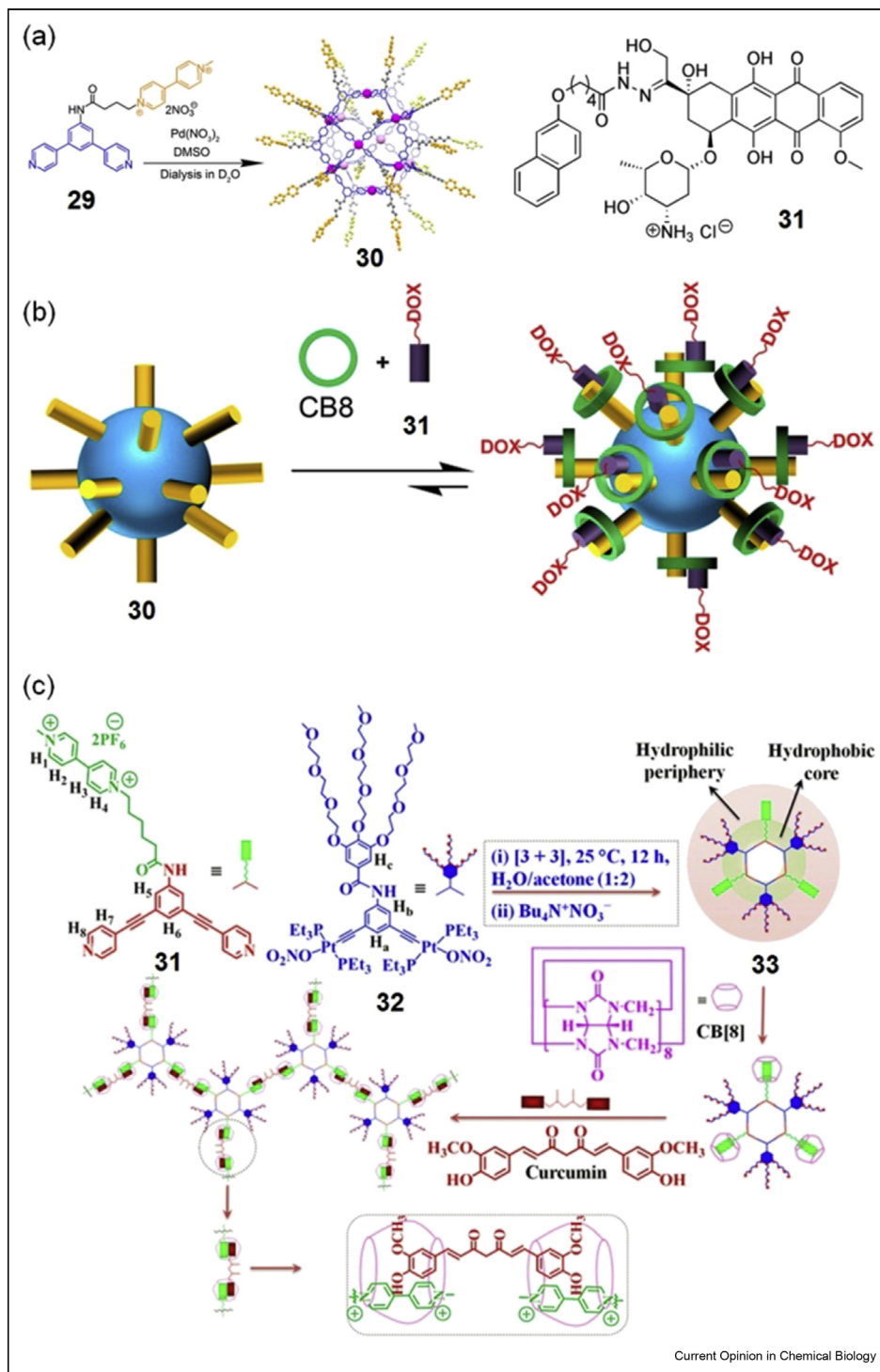
host–guest complex facilitated cellular internalization. Active cisplatin was efficiently released inside the cancer cells through a reduction reaction by biological reductants such as ascorbic acid, thus activating the anti-cancer ability. Yue et al. [65] constructed another host–guest complex using this cage as the host and a Pt(IV) prodrug (**27**) with a fluorescein tail as the guest in a 1:1 ratio with  $\mu\text{M}$  dissociation constants (Figure 5c). The inclusion complex was loaded into the nanoparticles using an anionic block copolymer (**28**) via electrostatic interactions (Figure 5b). The active anti-cancer drug released slowly from the nanoparticles, and the efficacy of this nanoformulation (half-inhibition concentration,  $IC_{50} = 5.02 \pm 0.67 \mu\text{M}$ ) was comparable with cisplatin ( $IC_{50} = 2.95 \pm 0.42 \mu\text{M}$ ) against HeLa cells. The introduction of targeting ligands on the SCCs

Figure 5



(a) Illustration of the host–guest complexation between the Pt(IV) prodrug (**26**) and the metallacage (**25**). Reproduced with permission from the study by Zheng et al. [64], copyright 2015 Royal Society of Chemistry. (b) Illustration of the nanoformulation strategy. (c) Illustration of the host–guest complexation between **25** and fluorescein and chromatic change of fluorescein upon binding to the metallacage. Reproduced with permission from the study by Yue et al. [65], copyright 2018 Royal Society of Chemistry.

Figure 6



(a) Chemical structure of the  $\text{Pd}_{12}\text{L}_{24}$  metallacage **30** and the prodrug **31**. (b) Cartoon illustration of the host-guest complexation. Reproduced with permission from the study by Samanta et al. [68], copyright 2016 American Chemical Society. (c) Chemical structure of the building blocks and cartoon illustration of the host-guest complexation. Reproduced with permission from the study by Datta et al. [69], copyright 2018 National Academy of Sciences. DOX, doxorubicin.

was a direct choice to elevate their therapeutic efficacy while alleviate the systemic toxicity by optimizing the biodistributions. Han et al. [66] modified the organic ligands by targeting groups for integrin  $\alpha_v\beta_3$  or  $\alpha_5\beta_1$  without affecting their coordination self-assembly. The IC<sub>50</sub> value of cisplatin decreased to half of the pristine drug by the formation of the host–guest complex with the resultant Pd<sub>2</sub>L<sub>4</sub> metallacage with the ability to deliver chemotherapeutics to A375 cells overexpressing  $\alpha_v\beta_3$  integrins. *Ex vivo* measurements further the hepatotoxicity and nephrotoxicity of cisplatin were attenuated on the basis of supramolecular chemistry and the active targeting strategy.

Yu et al. [43] and Therrien [67] developed 3D Ru(II) and Pt(II) metallacages and, respectively, used them as hosts to complex porphyrin-based photosensitizers. The metallacages not only protected the photosensitizers from light during the transport, but also facilitated their delivery to cancer cells. The host–guest recognition improved the dispersion of photosensitizers in physiologic environment, thus realizing synergistic anticancer effect to overcome drug resistance encountered by the platinum-based drugs. Samanta et al. [68] and Datta et al. [69] conjugated 4,4'-bipyridinium to the metallacages and used these platforms as supramolecular guests (Figure 6). The prodrug or active drug could be loaded through host–guest chemistry using cucurbit[8]uril (CB8) as the host by forming 1:1:1 ternary complexes (Figure 6b and c). *In vitro* studies demonstrated these supramolecular systems displayed exciting anticancer results. For example, the inclusion complex displayed ~100-fold anticancer efficacy relative to free curcumin against various cancer cell lines, including C32, B16F10, MCF-7, and MDA-MB231 [69].

## Conclusion

The past decades have witnessed the progress of SCCs in biomedical applications, especially in cancer theranostics. By regulating the functions of the individual building blocks and the geometry of their linkages, diverse nanomaterials with unique and enhanced properties can be prepared. The bioactive nature of the metals or metal complexes also determine the final functions of the SCCs, for example, the widely used Pt and Ru precursors hold excellent anticancer ability. Imaging probes can be incorporated into the SCCs, making the delivery and distribution of the SCCs visible. The therapeutic performance of the SCCs is substantially improved by introducing other modalities through covalent and noncovalent methods, which provide potential ways to overcome drug resistance. The solubility and stability of the SCCs in physiological media are the main obstacles for their *in vivo* uses, which can be effectively solved by the introduction of organometallic units into the supramolecular scaffolds and

nanotechnology. The pharmacokinetic behaviors including circulation halftime and tissue distributions are optimized by the formation of nanoformulations, greatly improving their antitumor performances and avoiding systemic toxicity, which paves the way for their clinic translation.

## Declaration of Competing Interest

The authors declare that they have no known competing financial interests or personal relationships that could have appeared to influence the work reported in this paper.

## Acknowledgements

This work was supported by the Intramural Research Program of the National Institute of Biomedical Imaging and Bioengineering, National Institutes of Health, and the National Natural Science Foundation of China (21434005, 21620102006).

## References

Papers of particular interest, published within the period of review, have been highlighted as:

- of special interest
  - of outstanding interest
1. Chabner BA, Roberts Jr TG: **Timeline: chemotherapy and the war on cancer.** *Nat Rev Canc* 2005, **5**:65–72.
  2. Chu KF, Dupuy DE: **Thermal ablation of tumours: biological mechanisms and advances in therapy.** *Nat Rev Canc* 2014, **14**: 199–208.
  3. Davoodi P, Lee LY, Xu Q, Sunil V, Sun Y, Soh S, et al.: **Drug delivery systems for programmed and on-demand release.** *Adv Drug Deliv Rev* 2018, **132**:104–138.
  4. Zhou J, Yu G, Huang F: **Supramolecular chemotherapy based on host-guest molecular recognition: a novel strategy in the battle against cancer with a bright future.** *Chem Soc Rev* 2017, **46**:7021–7053.
  5. Shi J, Kantoff PW, Wooster R, Farokhzad OC: **Cancer nanomedicine: progress, challenges and opportunities.** *Nat Rev Canc* 2017, **17**:20–37.
  6. Muthu MS, Leong DT, Mei L, Feng S: **Nanotheranostics-application and further development of nanomedicine strategies for advanced theranostics.** *Theranostics* 2014, **4**:660–677.
  7. Chen H, Zhang W, Zhu G, Xie J, Chen X: **Rethinking cancer nanotheranostics.** *Nat Rev Mater* 2017, **2**:17024.
  8. Jo S, Ku SH, Won Y, Kim SH, Kwon IC: **Targeted nanotheranostics for future personalized medicine: recent progress in cancer therapy.** *Theranostics* 2016, **6**:1362–1377.
  9. Panwar N, Soehartono AM, Chan KK, Zeng S, Xu G, Qu J, et al.: **Nanocarbons for biology and medicine: sensing, imaging, and drug delivery.** *Chem Rev* 2019, **119**:9559–9656.
  10. Yu G, Chen X: **Host-guest chemistry in supramolecular theranostics.** *Theranostics* 2019, **9**:3041–3074.
  11. Yu G, Yang Z, Fu X, Yung BC, Yang J, Mao Z, et al.: **Polyrotaxane-based supramolecular theranostics.** *Nat Commun* 2018, **9**:766.
  12. Kojima R, Aibel D, Fussenegger M: **Novel theranostic agents for next-generation personalized medicine: small molecules, nanoparticles, and engineered mammalian cells.** *Curr Opin Chem Biol* 2015, **28**:29–38.
  13. Johnstone TC, Suntharalingam K, Lippard SJ: **The next generation of platinum drugs: targeted Pt(II) agents, nanoparticle delivery, and Pt(IV) prodrugs.** *Chem Rev* 2016, **116**: 3436–3486.

14. Barry NP, Sadler PJ: **Challenges for metals in medicine: how nanotechnology may help to shape the future.** *ACS Nano* 2013, **7**:5654–5659.
15. Muhammad N, Guo Z: **Metal-based anticancer chemotherapeutic agents.** *Curr Opin Chem Biol* 2014, **19**:144–153.
16. Wang X, Wang X, Jin S, Muhammad N, Guo Z: **Stimuli-responsive therapeutic metallodrugs.** *Chem Rev* 2019, **119**:1138–1192.
17. Ahmedova A: **Biomedical Applications of metallosupramolecular assemblies-structural aspects of the anticancer activity.** *Front Chem* 2018, **6**:620.
18. Casini A, Woods B, Wenzel M: **The promise of self-assembled 3D supramolecular coordination complexes for biomedical applications.** *Inorg Chem* 2017, **56**:14715–14729.
19. Cook TR, Vajpayee V, Lee MH, Stang PJ, Chi KW: **Biomedical and biochemical applications of self-assembled metallacycles and metallacages.** *Acc Chem Res* 2013, **46**:2464–2474.
20. Northrop BH, Yang HB, Stang PJ: **Coordination-driven self-assembly of functionalized supramolecular metallacycles.** *Chem Commun (Camb)* 2008:5896–5908.
21. Li B, He T, Fan Y, Yuan X, Qiu H, Yin S: **Recent developments in the construction of metallacycle/metallacage-cored supramolecular polymers via hierarchical self-assembly.** *Chem Commun (Camb)* 2019, **55**:8036–8059.
22. McKinlay AC, Morris RE, Horcajada P, Ferey G, Gref R, Couvreur P, *et al.*: **BioMOFs: metal-organic frameworks for biological and medical applications.** *Angew Chem Int Ed* 2010, **49**:6260–6266.
23. Pothig A, Casini A: **Recent developments of supramolecular metal-based structures for applications in cancer therapy and imaging.** *Theranostics* 2019, **9**:3150–3169.
24. Sepehrpour H, Fu W, Sun Y, Stang PJ: **Biomedically relevant self-assembled metallacycles and metallacages.** *J Am Chem Soc* 2019, **141**:14005–14020.
- A great review summarized the recent advances of self-assembled metallacycles and metallacages relevant to biomedical applications.
25. Woods B, Dollerer D, Aikman B, Wenzel MN, Sayers EJ, Kuhn FE, *et al.*: **Highly luminescent metallacages featuring bispyridyl ligands functionalised with BODIPY for imaging in cancer cells.** *J Inorg Biochem* 2019, **199**:110781.
26. Gupta G, Das A, Panja S, Ryu JY, Lee J, Mandal N, *et al.*: **Self-assembly of novel thiophene-based BODIPY Ru(II) rectangles: potential antiproliferative agents selective against cancer cells.** *Chem Eur J* 2017, **23**:17199–17203.
27. Gupta G, Das A, Park KC, Tron A, Kim H, Mun J, *et al.*: **Self-assembled novel BODIPY-based palladium supramolecules and their cellular localization.** *Inorg Chem* 2017, **56**:4615–4621.
28. Zhou J, Zhang Y, Yu G, Crawley MR, Fulong CRP, Friedman AE, *et al.*: **Highly emissive self-assembled BODIPY-platinum supramolecular triangles.** *J Am Chem Soc* 2018, **140**:7730–7736.
- BODIPY-based ligand was utilized to construct theranostic metallacycle for living cell imaging and synergistic chemo-phototherapy.
29. Ma L, Yang T, Zhang Z, Yin S, Song Z, Shi W, *et al.*: **Cyanosilbene-based near-infrared emissive platinum (II) metallacycles for cancer theranostics.** *Chin Chem Lett* 2019, **30**:1942–1946.
30. Mei J, Leung NL, Kwok RT, Lam JW, Tang BZ: **Aggregation-induced emission: together we shine, united we soar!** *Chem Rev* 2015, **115**:11718–11940.
31. Ding D, Li K, Liu B, Tang BZ: **Bioprobes based on AIE fluorogens.** *Acc Chem Res* 2013, **46**:2441–2453.
32. Yan X, Cook TR, Wang P, Huang F, Stang PJ: **Highly emissive platinum(II) metallacages.** *Nat Chem* 2015, **7**:342–348.
33. Yan X, Wang H, Hauke CE, Cook TR, Wang M, Saha ML, *et al.*: **A suite of tetraphenylethylene-based discrete organoplatinum(II) metallacycles: controllable structure and stoichiometry, aggregation-induced emission, and nitroaromatics sensing.** *J Am Chem Soc* 2015, **137**:15276–15286.
34. Zheng W, Yang G, Jiang S-T, Shao N, Yin G-Q, Xu L, *et al.*: **A tetraphenylethylene (TPE)-based supra-amphiphilic organoplatinum (II) metallacycle and its self-assembly behaviour.** *Mater Chem Front* 2017, **1**:1823–1828.
35. Zhang M, Li S, Yan X, Zhou Z, Saha ML, Wang Y-C, *et al.*: **Fluorescent metallacycle-cored polymers via covalent linkage and their use as contrast agents for cell imaging.** *Proc Natl Acad Sci U S A* 2016, **113**:11100–11105.
36. Yu G, Cook TR, Li Y, Yan X, Wu D, Shao L, *et al.*: **Tetraphenylethylene-based highly emissive metallacage as a component of theranostic supramolecular nanoparticles.** *Proc Natl Acad Sci U S A* 2016, **113**:13720–13725.
37. Yu G, Yu S, Saha ML, Zhou J, Cook TR, Yung BC, *et al.*: **A discrete organoplatinum (II) metallacage as a multimodality theranostic platform for cancer photochemotherapy.** *Nat Commun* 2018, **9**:5712.
- The metallacage-loaded nanoparticles allowed trimodal imaging capability (NIR fluorescence, MRI and PET imaging) for precise diagnosis of tumor and real-time monitoring of the delivery. The combination of Pt-based chemotherapy and porphyrin-based photodynamic therapy exhibited superb anti-tumor performance and anti-metastasis effect.
38. Sun Y, Ding F, Zhou Z, Li C, Pu M, Xu Y, *et al.*: **Rhomboidal Pt (II) metallacycle-based NIR-II theranostic nanoprobe for tumor diagnosis and image-guided therapy.** *Proc Natl Acad Sci U S A* 2019, **116**:1968–1973.
39. Ding F, Chen Z, Kim WY, Sharma A, Li C, Ouyang Q, *et al.*: **A nano-cocktail of an NIR-II emissive fluorophore and organoplatinum(II) metallacycle for efficient cancer imaging and therapy.** *Chem Sci* 2019, **10**:7023–7028.
40. Sun Y, Ding F, Chen Z, Zhang R, Li C, Xu Y, *et al.*: **Melanin-dot-mediated delivery of metallacycle for NIR-II/ photoacoustic dual-modal imaging-guided chemo-photothermal synergistic therapy.** *Proc Natl Acad Sci U S A* 2019, **116**:16729–16735.
- NIR II fluorophore and chemotherapeutic metallacycle were encapsulated into the melanin dot, allowing dual-modal image-guided chemo-photothermal synergistic therapy.
41. Freudenreich J, Dalvit C, Süß-Fink G, Therrien B: **Encapsulation of photosensitizers in hexa- and octanuclear organometallic cages: synthesis and characterization of carceplex and host-guest systems in solution.** *Organometallics* 2013, **32**:3018–3033.
42. Garci A, Mbakidi J-P, Chaleix V, Sol V, Orhan E, Therrien B: **Tunable arene ruthenium metallaprisms to transport, shield, and release porphyrin in cancer cells.** *Organometallics* 2015, **34**:4138–4146.
43. Yu G, Zhu B, Shao L, Zhou J, Saha ML, Shi B, *et al.*: **Host-guest complexation-mediated codelivery of anticancer drug and photosensitizer for cancer photochemotherapy.** *Proc Natl Acad Sci U S A* 2019, **116**:6618–6623.
- The host-guest complex was used as a theranostic core for the preparation of nanomedicine for image-guided chemo-phototherapy with excellent synergy.
44. Burke BP, Grantham W, Burke MJ, Nichol GS, Roberts D, Renard I, *et al.*: **Visualizing kinetically robust Co<sup>II</sup><sub>4</sub>L<sub>6</sub> assemblies in vivo: SPECT imaging of the encapsulated [<sup>99m</sup>Tc] TcO<sub>4</sub><sup>-</sup> anion.** *J Am Chem Soc* 2018, **140**:16877–16881.
- The metallacage with high stability was employed as a supramolecular host to complex a radioactive tracer for SPECT imaging.
45. Gupta G, Nowak-Sliwinska P, Herrero N, Dyson PJ, Therrien B: **Increasing the selectivity of biologically active tetranuclear arene ruthenium assemblies.** *J Organomet Chem* 2015, **796**:59–64.
46. Vajpayee V, Song YH, Yang YJ, Kang SC, Cook TR, Kim DW, *et al.*: **Self-assembly of cationic, hetero- or homonuclear ruthenium (II) macrocyclic rectangles and their photo-physical, electrochemical, and biological studies.** *Organometallics* 2011, **30**:6482–6489.
47. Dubey A, Min JW, Koo HJ, Kim H, Cook TR, Kang SC, *et al.*: **Anticancer potency and multidrug-resistant studies of self-**

- assembled arene-ruthenium metallarectangles. *Chem Eur J* 2013, **19**:11622–11628.
48. Jo J-H, Singh N, Kim D, Cho SM, Mishra A, Kim H, *et al.*: **Coordination-Driven self-assembly using ditopic pyridyl-pyrazolyl donor and *p*-cymene Ru(II) acceptors: [2]catenane synthesis and anticancer activities.** *Inorg Chem* 2017, **56**: 8430–8438.
  49. Mishra A, Jung H, Park JW, Kim HK, Kim H, Stang PJ, *et al.*: **Anticancer activity of self-assembled molecular rectangles via arene-ruthenium acceptors and a new unsymmetrical amide ligand.** *Organometallics* 2012, **31**:3519–3526.
  50. Vajpayee V, Yang YJ, Kang SC, Kim H, Kim IS, Wang M, *et al.*: **Hexanuclear self-assembled arene-ruthenium nano-prismatic cages: potential anticancer agents.** *Chem Commun (Camb)* 2011, **47**:5184–5286.
  51. Mishra A, Jeong YJ, Jo JH, Kang SC, Lah MS, Chi KW: **Anti-cancer potency studies of coordination driven self-assembled arene-Ru-based metalla-bowls.** *ChemBiochem* 2014, **15**:695–700.
  52. Zhao Y, Zhang L, Li X, Shi Y, Ding R, Teng M, *et al.*: **Self-assembled ruthenium (II) metallacycles and metallacages with imidazole-based ligands and their in vitro anticancer activity.** *Proc Natl Acad Sci U S A* 2019, **116**:4090–4098.
  53. Mishra A, Chang Lee S, Kaushik N, Cook TR, Choi EH, Kumar Kaushik N, *et al.*: **Self-assembled supramolecular hetero-bimetallic cycles for anticancer potency by intracellular release.** *Chem Eur J* 2014, **20**:14410–14420.
  54. McNeill SM, Preston D, Lewis JE, Robert A, Knerr-Rupp K, Graham DO, *et al.*: **Biologically active [Pd<sub>2</sub>L<sub>4</sub>]<sup>4+</sup> quadruply-stranded helicates: stability and cytotoxicity.** *Dalton Trans* 2015, **44**:11129–11136.
  55. Grishagin IV, Pollock JB, Kushal S, Cook TR, Stang PJ, Olenyuk BZ: **In vivo anticancer activity of rhomboidal Pt(II) metallacycles.** *Proc Natl Acad Sci U S A* 2014, **111**: 18448–18453.
  56. Yue Z, Wang H, Li Y, Qin Y, Xu L, Bowers DJ, *et al.*: **Coordination-driven self-assembly of a Pt(IV) prodrug-conjugated supramolecular hexagon.** *Chem Commun (Camb)* 2018, **54**: 731–734.
  57. Zhou Z, Liu J, Rees TW, Wang H, Li X, Chao H, *et al.*: **Hetero-metallic Ru-Pt metallacycle for two-photon photodynamic therapy.** *Proc Natl Acad Sci U S A* 2018, **115**:5664–5669.
  58. Yao Y, Zhao R, Shi Y, Cai Y, Chen J, Sun S, Zhang W, Tang R: **2D amphiphilic organoplatinum(II) metallacycles: their syntheses, self-assembly in water and potential application in photodynamic therapy.** *Chem Commun (Camb)* 2018, **54**: 8068–8071.
  59. Zhou Z, Liu J, Huang J, Rees TW, Wang Y, Wang H, Li X, Chao H, Stang PJ: **A self-assembled Ru-Pt metallacage as a lysosometargeting photosensitizer for 2-photon photodynamic therapy.** *Proc Natl Acad Sci U S A* 2019, **116**: 20296–20302.
  60. Brabec V, Howson SE, Kaner RA, Lord RM, Malina J, Phillips RM, *et al.*: **Metallohelices with activity against cisplatin-resistant cancer cells; does the mechanism involve DNA binding?** *Chem Sci* 2013, **4**:4407–4416.
  61. Faulkner AD, Kaner RA, Abdallah QMA, Clarkson G, Fox DJ, Gurnani P, *et al.*: **Asymmetric triplex metallohelices with high and selective activity against cancer cells.** *Nat Chem* 2014, **6**: 797–803.
  62. Yu G, Zhang M, Saha ML, Mao Z, Chen J, Yao Y, *et al.*: **Antitumor activity of a unique polymer that incorporates a fluorescent self-assembled metallacycle.** *J Am Chem Soc* 2017, **139**:15940–15949.
  63. Qin Y, Chen LJ, Dong F, Jiang ST, Yin GQ, Li X, *et al.*: **Light-controlled generation of singlet oxygen within a discrete dual-stage metallacycle for cancer therapy.** *J Am Chem Soc* 2019, **141**:8943–8950.
- The generation of singlet oxygen was intelligently controlled by light using a dual-stage metallacage as the theranostic core, realizing precise photodynamic therapy.
64. Zheng YR, Suntharalingam K, Johnstone TC, Lippard SJ: **Encapsulation of Pt(IV) prodrugs within a Pt(II) cage for drug delivery.** *Chem Sci* 2015, **6**:1189–1193.
  65. Yue Z, Wang H, Bowers DJ, Gao M, Stilgenbauer M, Nielsen F, *et al.*: **Nanoparticles of metal-organic cages designed to encapsulate platinum-based anticancer agents.** *Dalton Trans* 2018, **47**:670–674.
  66. Han J, Räder AFB, Reichart F, Aikman B, Wenzel MN, Woods B, *et al.*: **Bioconjugation of supramolecular metallacages to integrin ligands for targeted delivery of cisplatin.** *Bioconjug Chem* 2018, **29**:3856–3865.
  67. Therrien B: **Transporting and shielding photosensitizers by using water-soluble organometallic cages: a new strategy in drug delivery and photodynamic therapy.** *Chem Eur J* 2013, **19**:8378–8386.
  68. Samanta SK, Moncelet D, Briken V, Isaacs L: **Metal-organic polyhedron capped with cucurbit[8]uril delivers doxorubicin to cancer cells.** *J Am Chem Soc* 2016, **138**:14488–14496.
  69. Datta S, Misra SK, Saha ML, Lahiri N, Louie J, Pan D, Stang PJ: **Orthogonal self-assembly of an organoplatinum(II) metallacycle and cucurbit[8]uril that delivers curcumin to cancer cells.** *Proc Natl Acad Sci U S A* 2018, **115**:8087–8092.